Engineering Failure Analysis 153 (2023) 107601

Contents lists available at ScienceDirect

Engineering Failure Analysis

journal homepage: www.elsevier.com/locate/engfailanal

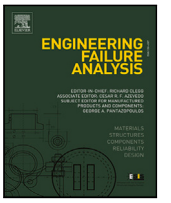

Failure analysis and retrofitting of reinforced concrete beams in existing moment resisting frames

F. Gusella *, M. Orlando

University of Florence, Department of Civil and Environmental Engineering, Via Santa Marta, 3 50139 Firenze, Italy

ARTICLE INFO

Keywords:
Civil engineering
Frame structures
Reinforced concrete
Limit analysis
Plastic mechanism
Failure load
Retrofitting

ABSTRACT

During the structure lifetime, the design loads can modify because of a changing in the use destination. In common practice, any architectural change of existing buildings, which modifies the magnitude of loads, requires the evaluation of the load-carrying capacity of structural members. To this aim a nonlinear analysis considering the rotation capacity of critical regions until the failure of the structure can be advantageous compared to a simple elastic analysis. Plastic deformations of ductile elements allow for attaining a more accurate evaluation of the ultimate load, once the strength of brittle mechanisms has been averted. Exploiting the actual rotation capacity of critical regions, where plastic hinges form, this paper presents new analytical closed-form equations to evaluate the ultimate load and the failure mode of an interior span of a multi-span moment resisting frame, as impacted by the strength of beam–column joints and the elastic and post-elastic structural response of adjacent elements. Taking advantage of derived equations, a retrofitting design procedure to identify the proper structural strengthening of critical regions is proposed. The accuracy of the method is checked through a comparison with numerical results. The procedure represents a new useful tool for engineers for the local strengthening of existing reinforced concrete buildings.

1. Introduction

The ultimate load of structures depends on both strength and ductility of members. The relevance to take into account the effective post-elastic behavior of Reinforced Concrete (R.C.) regions in structural analysis has been fully recognized [1–7] and current codes provide closed-form equations to evaluate the chord rotation capacity of sections [8,9]. The importance to know the failure mechanisms, the safety margins and the critical zones of structures is well recognized [10,11]. In addition to the assessment of the failure mode of RC systems, innovative techniques have been presented for the progressive collapse mitigation of RC frames [12,13], taking also into account seismic action [14].

The structural performance of Moment Resisting Frame (MRF) structures is influenced by the mechanical features of beam–column joints [15]. If on one hand for new structures, according to the capacity design, the shear collapse of beam–column joints is prevented [16] allowing beam–column joints to be assumed rigid and infinitely resistant, on the other hand, particular attention is required for existing concrete buildings, usually designed for vertical loads [17].

Several studies have been performed to evaluate the post-elastic response of R.C. members [18,19] and beam–column joints [20–23]. Plastic analysis, taking advantage of the redistribution of moments, allows for the load-carrying capacity of the structure to increase, leading to more efficient use of the material [24].

* Corresponding author.
E-mail addresses: federico.gusella@unifi.it (F. Gusella), maurizio.orlando@unifi.it (M. Orlando).

https://doi.org/10.1016/j.engfailanal.2023.107601
Received 7 March 2023; Received in revised form 4 August 2023; Accepted 1 September 2023
Available online 6 September 2023

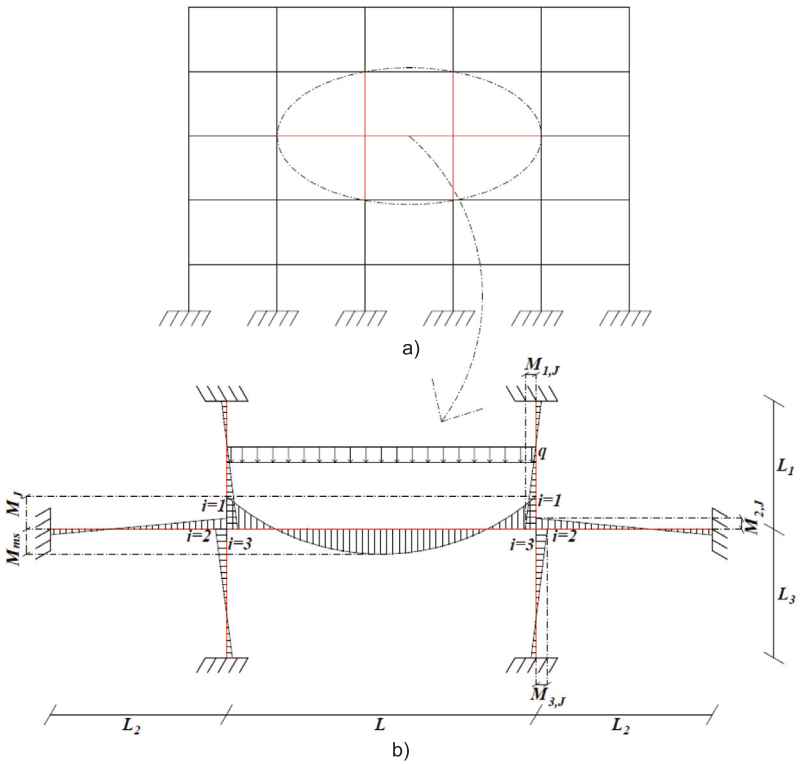

Fig. 1. (a) Multi-span multi-level Moment-Resisting-Frame, (b) Model adopted to analyze the structural response of an interior span.

The plastic behavior of R.C. members can be predicted by Finite Element (FE) numerical models: in implicit models, the stiffness and strength loss due to member damage is modeled by using nonlinear springs at the member sections [25–27]; in explicit models, each element is described considering several aspects of the inelastic mechanisms governing the element behavior [28–38]. Explicit models provide useful information about the effective structural performance of members and the influence of design parameters; implicit models allow to easily perform a plastic analysis of whole structures.

Although a nonlinear analysis can be performed through FE numerical models, this modeling approach requires a large data set for the calibration, in addition to computational resources. Vice-versa the designer needs a method that, starting from the mechanical properties of members, allows an easy prediction of the failure mode and the ultimate load of the structure [39], providing useful information about the proper structural strengthening strategy to increase the load-carrying capacity. Recent studies have been carried out to estimate the rotation of sections, which undergo plastic deformation, at failure [40]. The rotation assessment has also been investigated taking into account the impact due to the uncertainty in the mechanical properties in [41].

In the context of the design of new structures, differently from previous studies, the proposed equations allow to evaluate, in closed form, the required rotation of critical regions to achieve the theoretical ultimate load, that is the ultimate load assured by perfectly plastic hinges. Regarding the structural assessment of existing structures, the proposed approach allows to evaluate the effective ultimate load as affected by the actual rotation capacity of critical regions, where plastic deformation occurs. Moreover, the brittle shear failure of beam–column joints and the structural behavior of adjacent members, in terms of stiffness, strength and ductility, are considered. Through the assessment of the effective load-carrying capacity of the structure related to different collapse mechanisms, the proposed method allows for identifying the proper retrofitting strengthening strategy to increase the load-carrying capacity, providing closed-form equations easily adopted by practitioners. To prove the reliability and use of the method, the paper concludes with an application to a case study. The accuracy is checked by a comparison with numerical results and recommendations for the designer are provided.

2. Failure analysis of reinforced concrete frames

2.1. Preliminary elastic analysis

At the beginning, the elastic response of the R.C. frame under a vertical load, shown in Fig. 1, has to be evaluated.

The moment distribution can be obtained by overlapping the structural behavior of a pinned beam loaded by the distributed vertical load q and by the M_J reaction moments at beam-end (a list of symbols is reported in Appendix C). Assuming Bernoulli–Euler

beam theory, neglecting the shear and axial deformation, indicating with L the beam's span, E the Young's modulus, and I the second moment of area of the beam's section, M_J can be evaluated by

$$M_J = \frac{qL^3}{12}\left(\frac{K_J}{K_J L + 2EI}\right) \tag{1}$$

In the previous equation, K_J is the overall elastic flexural stiffness at the node due to the adjacent elements $i = 1, 2, 3$

$$K_J = \sum_{i=1}^{3} k_i = \sum_{i=1}^{3} \frac{4EI_i}{L_i}$$

where I_i and L_i are second moment of area and length of the upper column ($i = 1$), adjacent beam ($i = 2$) and bottom column ($i = 3$), Fig. 1.

The bending moment at beam mid-span can be obtained by

$$M_{ms} = \frac{qL^2}{8} - \frac{qL^3}{12}\left(\frac{K_J}{K_J L + 2EI}\right) = \frac{qL^2}{8}\left[1 - \frac{2}{3}\left(\frac{K_J L}{K_J L + 2EI}\right)\right] =$$
$$= \frac{qL^2}{8}\left[\frac{K_J L + 6EI}{3\left(K_J L + 2EI\right)}\right] = \frac{M_J}{2}\left(1 + \frac{6EI}{K_J L}\right) = M_J \psi$$

with

$$\psi = \frac{1}{2}\left(1 + \frac{6EI}{K_J L}\right)$$

$$M_J = \frac{M_{ms}}{\psi} = \frac{2M_{ms}}{\left(1 + 6EI/K_J L\right)} \tag{2}$$

Regarding elements $i = 1, 2, 3$, Fig. 1, the moments at element-end, close to the joint, are

$$M_{i,J} = \rho_i M_J \tag{3}$$

where ρ_i is

$$\rho_i = \frac{k_i}{K_J} = \frac{\frac{4EI_i}{L_i}}{K_J} = \frac{\frac{I_i}{L_i}}{\sum_{r=1}^{3} \frac{I_r}{L_r}}$$

2.2. First overcoming of the elastic phase by plastic hinge

The vertical load producing the elastic phase overcoming, with the formation of the first plastic hinge on the beam, is evaluated in the following.

Let $M_{J,u}$ be the ultimate moment at the beam-ends, and $M_{ms,u}$ the ultimate moment at the beam mid-span.

Then the load $q_{J,u}$, which produces the first plastic hinge at beam-ends and the load $q_{ms,u}$, which produces the first plastic hinge at mid-span, are respectively

$$q_{J,u} = \frac{12M_{J,u}}{L^3}\left(\frac{K_J L + 2EI}{K_J}\right) \tag{4}$$

$$q_{ms,u} = \frac{8M_{ms,u}}{L^2}\left(\frac{3K_J L + 6EI}{K_J L + 6EJ}\right) \tag{5}$$

It should be noted that the first hinge could form on the element $i = 1, 2, 3$ at the section adjacent to the node. Let $M_{i,J,u}$ be the ultimate moment of the element $i = 1, 2, 3$.

We introduce $M_{w,J,u}$ the ultimate moment at the beam-end relative to the collapse of the weakest adjacent element. Taking into account Eq. (3), we have

$$M_{w,J,u} = \min\left\{\frac{M_{i,J,u}}{\rho_i}\right\} = \min\left\{M_{i,J,u}\frac{K_J}{k_i}\right\} \quad i = 1, 2, 3$$

so that $q_{w,J,u}$, the load that produces the first plastic hinge at the weakest adjacent element, is

$$q_{w,J,u} = \frac{12M_{w,J,u}}{L^3}\left(\frac{K_J L + 2EI}{K_J}\right) \tag{6}$$

2.3. Shear failure of the beam–column joint

Beam–column joints of existing reinforced concrete structures are often the weakest element because of the shear failure.

Let V_u be the beam–column joint ultimate shear. The ultimate shear force of the joint can be evaluated by following equations [17]

$$\sigma_{nt} = \left| \frac{N}{2A_g} - \sqrt{\left(\frac{N}{2A_g}\right)^2 + \left(\frac{V_u}{A_g}\right)^2} \right| \leq 0.3\sqrt{f_c}$$

$$\sigma_{nc} = \left| \frac{N}{2A_g} + \sqrt{\left(\frac{N}{2A_g}\right)^2 + \left(\frac{V_u}{A_g}\right)^2} \right| \leq 0.5 f_c$$

that represent the required conditions on the maximum tensile stress and compressive stress on the joint required by design code, where N is the axial force acting on the upper column, A_g is the gross area of the joint panel horizontal section, f_c is the concrete compressive strength (in MPa). In particular, V_u is the smaller value obtained from previous equations assuming $\sigma_{nt} = 0.3\sqrt{f_c}$ and $\sigma_{nc} = 0.5 f_c$.

The joint shear V_J can be expressed by

$$V_J = \frac{M_J}{d_l} - \frac{M_2}{d_l} - V_1$$

where V_1 is the shear in the upper column and d_l is the beam lever arm, assumed equal for all elements.

The effect of the upper column shear is negligible; so that, considering that $M_2 = M_J k_2 / K_J$, we obtain

$$V_J = \frac{M_J}{d_l} - \frac{M_J k_2}{d_l K_J} = \frac{M_J}{d_l}\left(1 - \rho_2\right)$$

We introduce the ultimate moment at the beam-end $M_{V,J,u}$ that corresponds to the node shear failure; this can be obtained by previous equation with $V_J = V_u$

$$M_{V,J,u} = \frac{V_u d_l}{\left(1 - \rho_2\right)}$$

So that, the load $q_{V,J,u}$ that produces the joint failure, can be obtained by

$$q_{V,J,u} = \frac{12 M_{V,J,u}}{L^3}\left(\frac{K_J L + 2EI}{K_J}\right) \tag{7}$$

The joint shear collapse plays a critical role in the response of frame structures; in fact, having a brittle behavior, this can be considered a failure condition. Differently to the joint collapse, beams have a ductile response; plastic hinges form and can provide a rotation capable to achieve a greater load-carrying capacity.

3. Required rotations to achieve the theoretical ultimate load

In the following, the required rotations to achieve the theoretical ultimate load are estimated. We assume that the adjacent elements do not reach the ultimate moment $M_{i,J,u}$, with $i = 1, 2, 3$.

3.1. First plastic hinge at the beam-end section

We assume that the first plastic hinges occur at the beam-ends. In this case:

$$q_{J,u} \leq \left[q_{ms,u}, q_{V,J,u}, q_{w,J,u}\right]$$

Indicating $M_{J,ms,u}$ the moment at the beam-end when the ultimate moment $M_{ms,u}$ at the beam mid-span is achieved, see Eq. (2),

$$M_{J,ms,u} = \frac{2M_{ms,u}}{\left(1 + 6EI/K_J L\right)}$$

the previous condition can be expressed as

$$M_{J,u} \leq \left[M_{J,ms,u}, M_{V,J,u}, M_{w,J,u}\right] \equiv \left[\frac{2M_{ms,u}}{\left(1 + 6EI/K_J L\right)}, M_{V,J,u}, M_{w,J,u}\right] \tag{8}$$

A second hinge can form at beam mid-span; applying limit analysis, the failure load is

$$q_f = \frac{8\left(M_{ms,u} + M_{J,u}\right)}{L^2} \tag{9}$$

Nevertheless the plastic design of the structure can be performed only if the beam-end rotation is not lower than:

$$\theta_{J,u} = \frac{q_f L^3}{24EI} - \frac{M_{J,u} L}{2EI} \tag{10}$$

and substituting the failure load, Eq. (9), we have

$$\theta_{J,u} = \frac{L}{6EI}\left(2M_{ms,u} - M_{J,u}\right) \tag{11}$$

The rotation is independent from the stiffness of adjacent elements.

3.2. First plastic hinge at the beam mid-span section

Assuming that the first hinge occurs at the beam mid-span, we have

$$q_{ms,u} \le \left[q_{J,u}, q_{V,J,u}, q_{w,J,u}\right]$$

or equivalently

$$\frac{2M_{ms,u}}{\left(1 + 6EI/K_J L\right)} \le \left[M_{J,u}, M_{V,J,u}, M_{w,J,u}\right] \tag{12}$$

Increasing the load we have two alternative failure modes. If $M_{J,u} < M_{V,J,u}$, then a second hinge forms at both ends of the beam. Vice-versa, if $M_{V,J,u} < M_{J,u}$, then the joint collapses.

At first, we consider a second hinge at the beam-ends. To evaluate the required rotation of the beam at mid-span $\theta_{ms,u}$ to perform a plastic design with the complete redistribution of the moment, it can be observed that from $q_{ms,u}$, that produces the first hinge at the beam mid-span, to q_f, that produces the failure of the structure with the second hinge at beam-end, the increment of the load is $\Delta q = q_f - q_{ms,u}$. In order to allow the moment redistribution, the rotation of the plastic hinge at the beam mid-span under the Δq, can be expressed by:

$$\theta_{ms,u} = \frac{\Delta q L^3}{24EI} + \frac{\Delta q L^2}{4K_J} = \frac{\Delta q L^2}{4}\left(\frac{K_J L + 6EI}{6K_J EI}\right) \tag{13}$$

where the first term is due to the elastic deformation of the beam and the second term is related to the joint flexibility.

Supposing $M_{J,u} < M_{V,J,u}$ the q_f failure load is given by Eq. (9) and, considering Eq. (5), we obtain

$$\Delta q = \frac{8\left(M_{ms,u} + M_{J,u}\right)}{L^2} - \frac{8M_{ms,u}}{L^2}\left(\frac{3K_J L + 6EI}{K_J L + 6EI}\right) =$$
$$= \frac{8}{L^2}\left[M_{J,u} - M_{ms,u}\left(\frac{2K_J L}{K_J L + 6EI}\right)\right]$$

So that, the required rotation is

$$\theta_{ms,u} = \left(\frac{2}{K_J} + \frac{L}{3EI}\right) M_{J,u} - \frac{2L}{3EI} M_{ms,u} \tag{14}$$

This result can be checked by a different approach, see Appendix A.

The following conditions have to be respected

$$M_{J,u}\rho_i < M_{i,u} \quad i = 1,2,3$$

Now we have consider the shear collapse of the joint, $M_{V,J,u} < M_{J,u}$; in this case the failure load q_f is

$$q_f = \frac{8\left(M_{ms,u} + M_{V,J,u}\right)}{L^2} \tag{15}$$

the required rotation is

$$\theta_{ms,u} = \left(\frac{2}{K_J} + \frac{L}{3EI}\right) M_{V,J,u} - \frac{2L}{3EI} M_{ms,u} \tag{16}$$

The following conditions have to be respected

$$M_{V,J,u}\rho_i < M_{i,u} \quad i = 1,2,3$$

3.3. Beam–column joint collapse

As previously noted, if the first element to collapse is the beam–column joint,

$$q_{V,J,u} \le \left[q_{J,u}, q_{ms,u}, q_{w,J,u}\right]$$

or equivalently

$$M_{V,J,u} \le \left[M_{J,u}, \frac{2M_{ms,u}}{1 + 6EI/K_J L}, M_{w,J,u}\right] \tag{17}$$

we have a brittle failure and the ultimate load can be expressed by Eq. (7).

4. Effective ultimate load as affected by the section rotation capacity

In the following the effective ultimate load as affected by the section rotation capacity is assessed. When the section, where first plastic hinge forms, can provide the required rotation, Eqs. (11), (14) and (16), we have the complete redistribution of the moment and the failure load is given by Eq. (9) or Eq. (15). Otherwise, the ultimate load is influenced by the section rotation effective capacity. The effective rotation can be estimated through the section curvature capacity taking into account the L_p plastic hinge length

$$\theta_{u,eff} = \left(\Theta_u - \Theta_y\right) L_p \tag{18}$$

where Θ_u is the ultimate curvature and Θ_y is the yield curvature.

If the first hinges form at beam-ends, the $q_{f,eff,J}$ effective failure load can be obtained by Eq. (10) substituting the effective rotation at the beam end $\theta_{J,u,eff}$

$$q_{f,eff,J} = \frac{24EI}{L^3}\left(\theta_{J,u,eff} + \frac{M_{J,u}L}{2EI}\right) = \frac{24EI\theta_{J,u,eff}}{L^3} + \frac{12M_{J,u}}{L^2} \tag{19}$$

If the first hinge forms at beam mid-span, the effective increment of load can be obtained by Eq. (13) substituting the beam mid-span effective rotation $\theta_{ms,u,eff}$

$$\Delta q_{eff} = \frac{4\theta_{ms,u,eff}}{L^2}\left(\frac{6K_J EI}{K_J L + 6EI}\right)$$

so that the effective failure load $q_{f,eff,ms}$ is

$$\begin{aligned} q_{f,eff,ms} &= q_{ms,u} + \Delta q_{eff} = \frac{8M_{ms,u}}{L^2}\left(\frac{3K_J L + 6EI}{K_J L + 6EI}\right) + \frac{4\theta_{ms,u,eff}}{L^2}\left(\frac{6K_J EI}{K_J L + 6EI}\right) = \\ &= \frac{24K_J EI}{L^2\left(K_J L + 6EI\right)}\left(M_{ms,u}\left(\frac{L}{EI} + \frac{2}{K_J}\right) + \theta_{ms,u,eff}\right) \end{aligned} \tag{20}$$

5. Retrofitting design procedure and application to a case study

5.1. Retrofitting design

An iterative design procedure for identifying the proper retrofitting intervention with the goal to achieve a target vertical load $q_{f,T}$ is proposed taking advantage from the closed-form equations previously determined. The start corresponds to identify the weakest component:

a — beam-end by Eq. (8),
b — beam mid-span by Eq. (12),
c — beam–column joint by Eq. (17),

Then it is possible to identify the relative failure load considering the section rotation capacity:

a — Eq. (19),
b — Eq. (20),
c — Eq. (7).

5.2. Case study

The validity and accuracy of the closed-form equations and proposed retrofitting procedure have been checked by a specific application. The case study is the existing building Santa Maria Annunziata Hospital, in Bagno a Ripoli near Florence (I). The hospital was designed in 1966 and built in 1968–1972, taking into account only vertical loads because of the lack of seismic standard code. The hospital complex is characterized by seven buildings. The Unit No. 1 has been considered. This Unit has a basement floor, four floors and a walkable roof; the plan of the structure is shown in Fig. 2.

The available design documentation and experimental tests allowed estimating the geometrical characteristics of concrete cross-sections and reinforcement bars. The geometric characteristics are reported in Table 1 where b is the cross-section width, h is the cross-section height and L is the member length.

By experimental tests, the average concrete compressive strength has been estimated $f_{cm} = 22,5\ \mathrm{N/mm^2}$, while the average yield strength of reinforcing bars $f_{ym} = 440,0\ \mathrm{N/mm^2}$.

Assuming the stress block model for the concrete and the linear elastic-perfectly plastic behavior for the steel, the ultimate moment of elements was estimated; the values are reported in Table 2.

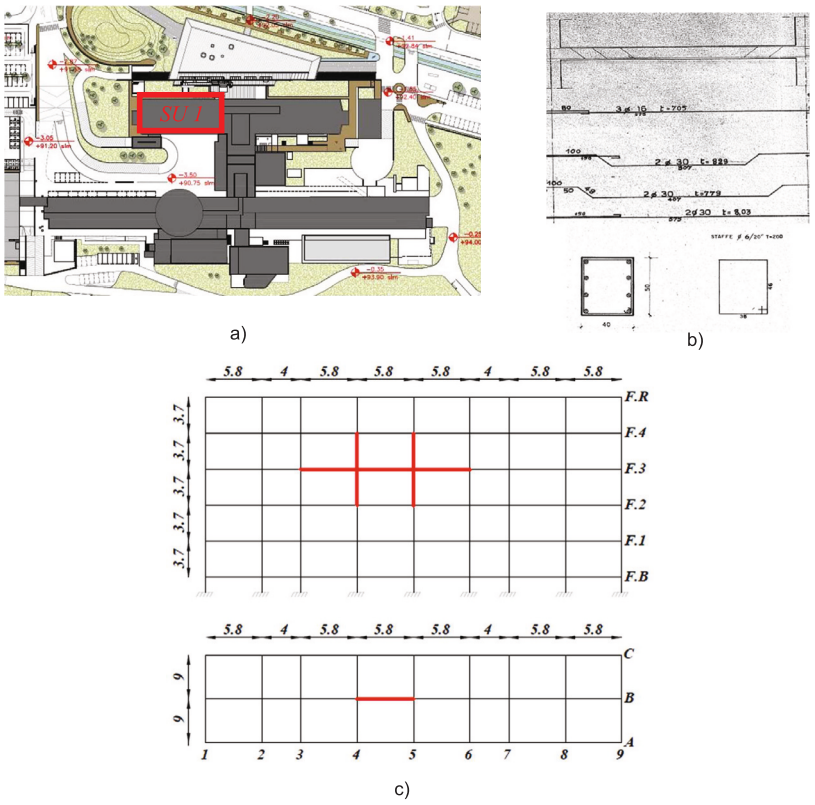

Fig. 2. (a) Plan of the Santa Maria Annunziata Hospital and identification of the case study: Structural Unit No. 1 (SU 1), (b) Extract from the existing structural drawings, (c) Multi-span multi-level Moment-Resisting-Frame of the SU 1, with the frame investigated in bold red (longitudinal section and plan).

Table 1
Geometric characteristics of elements (mm).

Characteristic	Top column	External beam	Bottom column	Internal beam
	i=1	i=2	i=3	
b	500	1200	500	1200
h	400	400	400	400
L	3700	5800	3700	5800

Table 2
Ultimate moments [kNm].

Beam-end	Beam mid-span	Beam–column joint	Top column	External beam	Bottom column
$M_{J,u}$	$M_{ms,u}$	$M_{V,J,u}$	$M_{1,u}$	$M_{2,u}$	$M_{3,u}$
545	230	147	212	545	242

5.3. Numerical model

To check the failure load and relative collapse mechanism, as estimated by the analytical procedure, a numerical model is adopted. A FE model of the frame structure, Fig. 2, is developed using the numerical code SAP 2000 [42]. One-dimensional elastic beam elements with lumped-plasticity are used. In particular, regarding the post-elastic response, a moment–rotation plastic curve, modeled by a rotational spring placed at the member-end, is adopted for the beam and adjacent elements. The curve is defined by the ultimate moment and the effective rotation of each member. The brittle shear failure of the beam–column joint is identified by the moment acting on the beam end $M_{V,J,u}$. In particular, a moment–rotation spring is placed in series with the spring simulating the response of the beam, at the intersection between the beam and the column, Fig. 3. Additional details of the numerical model and its capacity to estimate the failure mechanism of R.C. structures, as impacted by an eventual brittle collapse of the beam–column joint, can be found in [17]. In particular, the numerical model was used to simulate the experimental tests on existing R.C. structures reported in [22]; the model provided the ultimate loads and displacements with a 2%–3% error with respect to the experimental tests.

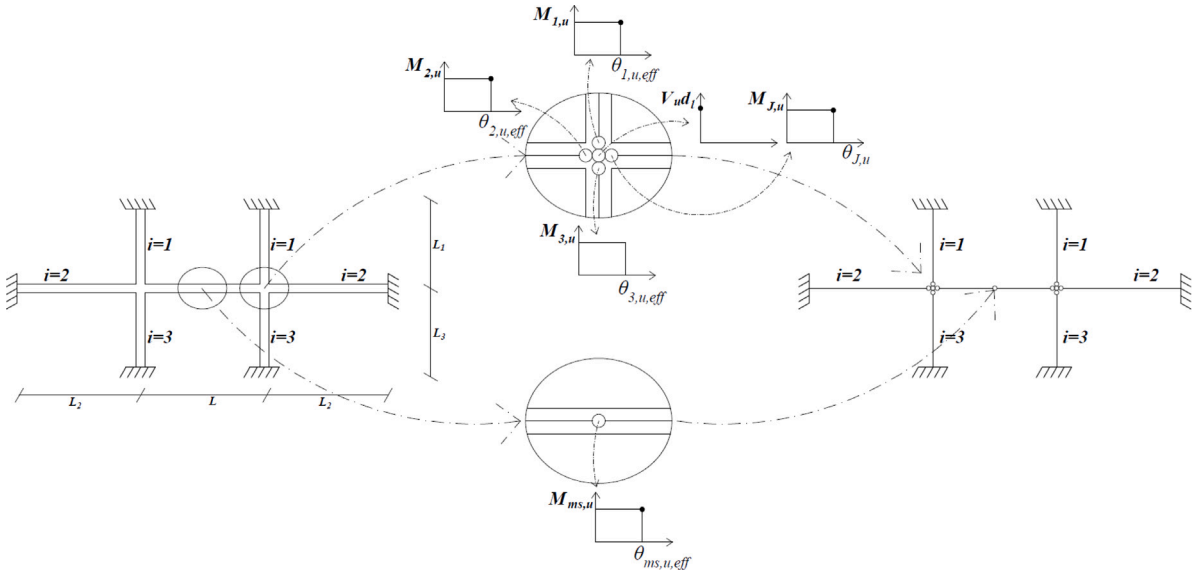

Fig. 3. Identification of the position and moment–rotation curve of hinges simulating the member behavior in the FE numerical model, (a) Moment-Resisting-Frame, (b) position of plastic hinges (springs) simulating the structural response of critical regions through moment–rotation curves, (c) scheme of the FE model.

5.4. Results for the case study

Starting from the existing structural configuration, (A — existing structure, Fig. 4), the failure load was $q_f = q_{V,J,u} = q_{f0} = 63,8$ kN/m and it corresponds to the brittle failure of the beam–column joint (the weakest component), Table 3. This results was checked by numerical analysis that provided a failure load $q_{f0,n} = 63,4$ kN/m. It should be observed that this value was a conservative assessment of the failure load because the confinement of joint, given by adjacent elements, was neglected.

We assume to strengthen the beam–column joint, $M_{V,J,u} = 600$ kNm. In this case (R1 — retrofitting phase 1) the first plastic hinge forms at the beam mid-span section and the failure mode is related to the effective ultimate rotation at that section; we have $\theta_{ms,u,eff} = 0,0020$ rad so that the failure load increases to $q_{f,eff,ms} = q_{f1} = 149,6$ kN/m. This result was checked by numerical analysis that provided a failure load $q_{f1,n} = 147,8$ kN/m.

The failure load $q_f = q_{f2} = 184,3$ kN/m can be achieved by increasing the rotation capacity at the beam mid-span (R2 — retrofitting phase 2). The numerical load was $q_{f2,n} = 183,3$ kN/m. The mechanism is given by the first hinge at mid-span and the second hinges at the beam-end. The analytical and numerical beam mid-span rotation was $\theta_{ms,u} = \theta_{ms,u,n} = 0,004$ rad.

The ultimate bending moment at the beam mid-span was increased to $M_{ms,J,u} = 545$ kNm (R3 — retrofitting phase 3). The first plastic hinge forms at beam-ends and the analytical failure load becomes $q_{f,eff,J} = q_{f3} = 241$ kN/m and the numerical one $q_{f3,n} = 240$ kN/m; this collapse mechanism is achieved when the effective rotation capacity is obtained at the beam-ends $\theta_{J,eff} = \theta_{J,eff,n} = 0.00198$ rad, where the first plastic hinges form.

Eventually, a structural strengthening at the beam-ends, capable to increase the rotation capacity is assumed (R4 — retrofitting phase 4). This allows to perform a complete redistribution of the moment with a second hinge at the beam mid-span, with a related ultimate load $q_f = q_{f4} = 259$ kN/m ($q_{f4,n} = 257$ kN/m); the rotation of the first plastic hinge at the joint was $\theta_{J,u} = 0,00274$. The obtained results are summarized in Table 3; the failure modes are shown in Fig. 4.

In particular the comparison between analytical and numerical results highlights the accuracy of the proposed approach, which can be adopted to estimate the effective load-carrying capacity of frame structures and, identifying the weakest component, suggests the proper structural reinforcement intervention in terms of strength and ductility for increasing the load-carrying capacity.

6. Influence of the adjacent elements on the failure mechanism

In the previous application, none of the adjacent elements (columns and beams $i = 1,2,3$) reached, at the node, the plastic condition. This situation is quite common; for example, if vertical loads are increased on all spans, the internal columns, with same length, are approximately stressed only by axial force. However it is possible that adjacent elements achieve the ultimate moment so that the related effects have to be considered because the rotational stiffness at the joint changes.

6.1. First elastic overcoming on the beam

At first, we reconsider the previously described failure mechanisms; in other words, we assume that the first hinge forms on the beam and the effects of an eventual failure of the adjacent elements is investigated.

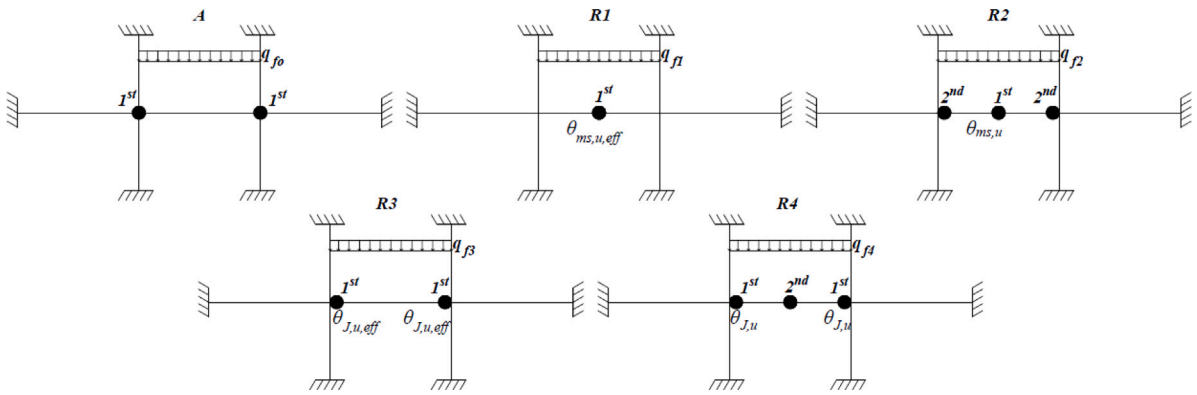

Fig. 4. Failure mechanisms for the existing structure (A) and the structure after a strengthening (Ri): hinge at beam mid-span (R1); hinges at beam mid-span and beam ends (R2); hinges at beam-ends (R3); hinges at beam-ends and beam mid-span (R4).

Table 3
Failure load and relative mode, (A) existing structure, (R_i $i = 1:4$) strengthening (dimension: failure load kN/m, rotation rad; n=numerical result).

Case	Failure mode
A	Beam–column joint collapse $q_{f0} = 63,8$ $q_{f0,n} = 63,4$ $q_{f0}/q_{f0,n} = 1,01$
R1	First hinge at beam mid-span with overcoming of plastic hinge rotation capacity $q_{f1} = 149.6$ $q_{f1,n} = 147.8$ $q_{f1}/q_{f1,n} = 1.01$ $\theta_{ms,u,eff} = 0.0020$
R2	First hinge at beam mid-span – second hinge at beam-ends $q_{f2} = 184.3$ $q_{f2,n} = 183,3$ $q_{f2}/q_{f2,n} = 1.01$ $\theta_{ms,u} = 0.00443$
R3	First hinge at beam-ends with overcoming of plastic hinges rotation capacity $q_{f3} = 241.3$ $q_{f3,n} = 240.3$ $q_{f3}/q_{f3,n} = 1.00$ $\theta_{J,u,eff} = 0.00198$
R4	First hinge at beam-ends – second hinge at beam mid-span $q_{f4} = 259.2$ $q_{f4,n} = 257.1$ $q_{f4}/q_{f4,n} = 1.01$ $\theta_{J,u} = 0.00274$

6.1.1. First plastic hinge forms at the beam-end section

If the first plastic hinge forms at the beam-end section (see paragraph 3.1); we note that, also increasing the load, there is not an increment of the moment at the node and plastic hinges in the adjacent elements will not form. Results of Section 3.1, not depending on the joint stiffness, do not undergo any changes.

6.1.2. First plastic hinge forms at the beam mid-span section

Now we consider that first plastic hinge forms at the mid-span section (see paragraph 3.2). In this case an increment of load can produce hinges in the elements adjacent to the joint; the degradation of the joint stiffness has to be considered to estimate the required rotation, see Appendix B.

– Case A: hinge on element $i = 1$ and collapse by hinge at the beam-end section. The q_f failure load is given by Eq. (9) and the overall required rotation is given by Eq. (A2.1)

– Case B: hinges on elements $i = 1,2$ and collapse by hinge at the beam-end section The q_f failure load is always given by Eq. (9) and the overall required rotation is given by Eq. (A2.2)

– Case C: hinges on elements $i = 1,2,3$ In this case the $q_{f,\bar{M}_R}$ failure load given by Eq. (A2.3) and the overall required rotation is given by Eq. (A2.5)

6.2. First hinges on the adjacent elements

We consider that the first hinge forms on the element, without loss of generality, $i = 1$. This situation changes the flexural stiffness at the beam–column joint, that is $K_J^{(1)}$, and the moment distribution in the beam. If the second hinge forms on the beam (beam-end or mid-span section)it is possible to use the analysis reported in the previous paragraph.

Vice versa, if the second forms on the element $i = 2$, the flexural stiffness at the beam–column joint changes to $K_J^{(1,2)}$ with analogous effects.

Moreover, if a third hinge forms on the element $i = 3$ we have the "joint rotation mechanism" that is equivalent to hinge at the beam-end section whit a moment $\bar{M}_R$, Eq. (A2.4).

It should be noted that in the previous we have supposed that the hinge rotation on the adjacent elements are provided, this should be checked. Moreover we have supposed that there is not the joint shear failure; this brittle mechanism should be verified.

Table 4
Plastic hinges on adjacent elements – Failure loads and relative mechanisms – Comparison with numerical results (dimension: moment kNm, failure load kN/m, rotation rad; n=numerical result).

Case	Failure mode
1	$M_{1,u} = 150,\ M_{2,u} = 300,\ M_{3,u} = 400,\ M_{J,u} = 700,\ M_{ms,u} = 800$ Hinges: $i = 3,2$ - beam-end section - beam mid-span section - Fig. 5 $q_f = 356,7,3\ q_{f,n} = 353,8,9\ q_{fo}/q_{fo,n} = 1,01$ $\theta_{J,u} = 0,00164\ \theta_{J,u,n} = 0,00157\ \theta_{J,u}/\theta_{Ju,n} = 1,04$
2	$M_{2,u} = 545,\ M_{3,u} = 150,\ M_{J,u} = 545,\ M_{ms,u} = 800$ Hinges: $i = 3$ - beam-end section - beam mid-span section - Fig. 5 $q_f = 319,9\ q_{f,n} = 317,4\ q_{fo}/q_{fo,n} = 1,01$ $\theta_{J,u} = 0,00233\ \theta_{J,u,n} = 0,00237\ \theta_{J,u}/\theta_{J,u,n} = 0,98$
3	$M_{2,u} = 545,\ M_{3,u} = 180,\ M_{J,u} = 545,\ M_{ms,u} = 230$ Hinges: beam mid-span section - $i = 3$ - beam-end section - Fig. 5 $q_f = 184,3\ q_{f,n} = 182,9\ q_{fo}/q_{fo,n} = 1,01$ $\theta_{ms,u} = 0,00637\ \theta_{ms,u,n} = 0,00651\ \theta_{ms,u}/\theta_{ms,u,n} = 0,98$

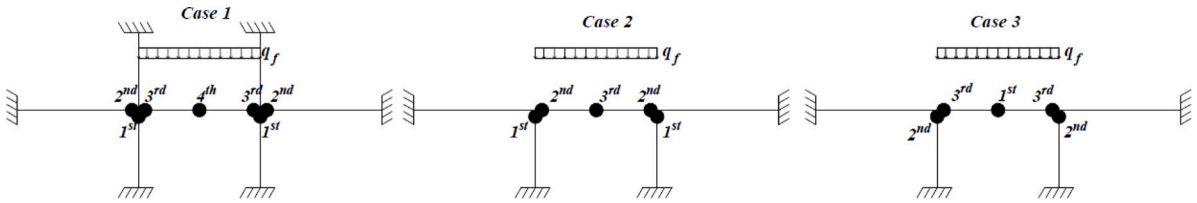

Fig. 5. Different failure mechanisms with plastic hinges on adjacent elements and identification of the hinge formation sequence.

6.3. Application to the case study

To check the previous analytical approach, a comparison with numerical simulation has been performed using the FE model previously described. Some examples are listed in Table 4, with the failure mechanisms shown in Fig. 5. Results highlighted the accuracy of proposed procedure in terms of both the failure load and required rotation (it should be noted that cases 2 and 3 have only bottom columns as they represent the structural scheme of the roof level).

7. Conclusions

An analytical framework capable to evaluate the failure load and associated collapse mechanism of an interior span of a moment-resisting-frame, considering the influence of adjacent members in terms of stiffness, strength, and ductility, in addition to the brittle failure of beam–column joints, is developed. The analytical assessment of the required rotation to achieve the theoretical ultimate load with the complete redistribution of the moment can be adopted for the design of new structures. The estimation of the effective load-carrying capacity of existing structures, as affected by the actual rotation capacity of critical regions, where plastic hinges form, represents a useful method for engineers to identify the proper structural strengthening to achieve a target vertical load. The method is based on a nonlinear analysis until the system failure and closed-form equations are provided to evaluate the critical regions and the effective ultimate load. For sake of simplicity, a symmetric structural scheme is investigated, and the member shear failure is not considered, as the eventual shear strengthening can be easily defined after the evaluation of the ultimate load related to the failure mechanism. To illustrate the use of the proposed approach, for the assessment and retrofitting of reinforced concrete existing buildings, a case study is discussed. The accuracy has been confirmed through the comparison with numerical results and the retrofitting design procedure is explained. The method shows that, as expected, the critical regions can be correctly estimated considering the flexural stiffness of adjacent members. The ultimate load is not affected by the stiffness of adjacent members if plastic hinges form first at the span-ends. Vice versa, if the first plastic hinge forms at the mid-span, and the last plastic hinges arise at the beam-ends at failure, the effective ultimate load cannot be accurately estimated by neglecting the flexural stiffness of adjacent members. The method can easily be adopted in common practice by designers to increase the vertical ultimate load, exploiting the local ductility where required and the strength without reducing the available global ductility.

Declaration of competing interest

The authors declare that they have no known competing financial interests or personal relationships that could have appeared to influence the work reported in this paper.

Data availability

No data was used for the research described in the article.

Appendix A

The rotation given by Eq. (14) can be also obtained by a global analysis. In fact, for a generic q load, the contributions of the load and $M_{ms,u}$ to the rotation are respectively

$$\theta_{ms,u}^{(q)} = 2\left(\frac{qL^3}{48EI} + \frac{qL^2}{8K_J}\right)$$

$$\theta_{ms,u}^{(M_{ms,u})} = -2\left(\frac{M_{ms,u}L}{2EI} + \frac{M_{ms,u}}{K_J}\right)$$

and

$$\theta_{ms,u}^{(q,M_{ms,u})} = qL^2\left(\frac{L}{24EI} + \frac{1}{4K_J}\right) - \left(\frac{L}{EI} + \frac{2}{K_J}\right)M_{ms,u}$$

When $M_J = M_{J,u}$, we have $q = q_f$, given by Eq (9), and substituting in the previous we obtain Eq. (14).

Appendix B

– Case A: hinge on element $i = 1$ and collapse by hinge at the beam-end section
Without loss generality, we assume that a hinge forms at the element $i = 1$, so that $M_{1,J} = \rho_1 M_J = M_{1,u}$.
The load to obtain this condition is

$$q^{(1)} = \frac{8\left(M_{1,u}/\rho_1 + M_{ms,u}\right)}{L^2}$$

This condition does not correspond to failure and the required rotation, from Eq. (14), is

$$\theta_{ms,u}^{(1)} = \left(\frac{L}{3EI} + \frac{2}{K_J}\right)\frac{M_{1,u}}{\rho_1} - \frac{2L}{3EI}M_{ms,u}$$

We suppose that a further increasing of the load $\Delta q^{(1,J)}$ gives a hinge at the joint section (in other words, plastic hinges do not form on the other elements $i = 2, 3$); this corresponds to the failure condition with the q_f failure load given by Eq. (9). To obtain this condition the increment of load is

$$\Delta q^{(1,J)} = q_f - q^{(1)} = \frac{8\left(M_{J,u} - M_{1,u}/\rho_1\right)}{L^2}$$

and the increment of the required rotation is

$$\Delta\theta_{ms,u}^{(1,J)} = \Delta q^{(1,J)}L^2\left(\frac{L}{24EI} + \frac{1}{4K_J^1}\right)$$

where $K_J^1 = k_2 + k_3$ is the new elastic flexural stiffness at the beam-to-column node. Substituting Δq we have

$$\Delta\theta_{ms,u}^{(1,J)} = \left(\frac{L}{3EI} + \frac{2}{K_J^1}\right)\left(M_{J,u} - \frac{M_{1,u}}{\rho_1}\right)$$

Hence the overall required rotation is

$$\theta_{ms,u}^{(1,J)} = \theta_{ms,u}^{(1)} + \Delta\theta_{ms,u}^{(1,J)} = \\ = \left(\frac{L}{3EI} + \frac{2}{K_J^1}\right)M_{J,u} - 2\left(\frac{1}{K_J^1} - \frac{1}{K_J}\right)\frac{M_{1,u}}{\rho_1} - \frac{2L}{3EI}M_{ms,u} \tag{A2.1}$$

– Case B: hinges on elements $i = 1, 2$ and collapse by hinge at the beam-end section
Now we suppose that, after the hinge formation on element $i = 1$, a hinge forms in element $i = 2$, and eventually the system collapses by hinge formation at the beam-end section. When the hinge forms on element $i = 1$ we have $M_{1,J} = M_{1,u}$ and $M_J = M_{1,u}/\rho_1$ so that $M_{2,J} = M_{1,u}(\rho_2/\rho_1)$ and $M_{3,J} = M_{1,u}(\rho_3/\rho_1)$. In order to have a hinge on element $i = 2$ the moment has to increase of

$$\Delta M_{2,J} = M_{2,u} - M_{1,u}\rho_2/\rho_1$$

and the beam-end moment has to increase of

$$\Delta M_J^{(1,2)} = (M_{2,u} - M_{1,u}\rho_2/\rho_1)/\tilde{\rho}_2$$

where $\tilde{\rho}_2 = I_2/L_2/(I_2/L_2 + I_3/L_3)$. So that the moment at the joint is

$$M_J^{(1,2)} = M_{1,u}/\rho_1 + \Delta M_J^{(1,2)} = M_{1,u}/\rho_1 + (M_{2,u} - M_{1,u}\rho_2/\rho_1)/\tilde{\rho}_2 = \\ = M_{1,u}/\rho_1\left(1 - \rho_2/\tilde{\rho}_2\right) + M_{2,u}/\tilde{\rho}_2$$

and the relative load is

$$q^{(1,2)} = 8\left(M_J^{(1,2)} + M_{ms,u}\right)/L^2$$

In this condition, the moment on element $i = 3$ is

$$\begin{aligned} M_{3,J} &= M_{1,u}(\rho_3/\rho_1) + \Delta M_J^{(1,2)}\tilde{\rho}_3 \\ &= M_{1,u}(\rho_3/\rho_1) + (M_{2,u} - M_{1,u}\rho_2/\rho_1)\left(\tilde{\rho}_3/\tilde{\rho}_2\right) \end{aligned}$$

where $\tilde{\rho}_3 = I_3/L_3/(I_2/L_2 + I_3/L_3)$.

The increment of load is

$$\Delta q^{(1,2)} = q^{(1,2)} - q^{(1)} = \frac{8\Delta M_J^{(1,2)}}{L^2} = \frac{8\left(M_{2,u} - M_{1,u}\rho_2/\rho_1\right)}{L^2\tilde{\rho}_2}$$

The increment of required rotation

$$\Delta\theta_{ms,u}^{(1,2)} = \Delta q^{(1,2)}L^2\left(\frac{L}{24EI} + \frac{1}{4K_J^1}\right) = \left(\frac{L}{3EI} + \frac{2}{K_J^1}\right)\frac{M_{2,u} - M_{1,u}\rho_2/\rho_1}{\tilde{\rho}_2}$$

so that the required rotation is

$$\begin{aligned} \theta_{ms,u}^{(1,2)} &= \theta_{ms,u}^{(1)} + \Delta\theta_{ms,u}^{(1,2)} = \\ &= \left(\frac{L}{3EI} + \frac{2}{K_J}\right)\frac{M_{1,u}}{\rho_1} + \left(\frac{L}{3EI} + \frac{2}{K_J^1}\right)\frac{M_{2,u} - M_{1,u}\rho_2/\rho_1}{\tilde{\rho}_2} - \frac{2L}{3EI}M_{ms,u} \end{aligned}$$

We suppose to increase the load until to obtain the failure with a hinge form at the beam-end section. The failure load is always given from Eq. (9).

In order to obtain this condition, the increment of beam-end section moment is

$$\begin{aligned} \Delta M_J^{(1,2,J)} &= M_{J,u} - M_J^{(1,2)} = M_{J,u} - \left(M_{1,u}/\rho_1 + (M_{2,u} - M_{1,u}\rho_2/\rho_1)/\tilde{\rho}_2\right) \\ &= M_{J,u} - M_{1,u}/\rho_1\left(1 - \rho_2/\tilde{\rho}_2\right) - M_{2,u}/\tilde{\rho}_2 \end{aligned}$$

whit an increment of load

$$\Delta q^{(1,2,J)} = \frac{8\Delta M_J^{(1,2,J)}}{L^2} = \frac{8\left(M_{J,u} - \left(M_{1,u}/\rho_1 + (M_{2,u} - M_{1,u}\rho_2/\rho_1)/\tilde{\rho}_2\right)\right)}{L^2}$$

and an increment of rotation

$$\begin{aligned} \Delta\theta_{ms,u}^{(1,2,J)} &= \Delta q^{(1,2,J)}L^2\left(\frac{L}{24EI} + \frac{1}{4K_J^{1,2}}\right) = \\ &= \left(\frac{L}{3EI} + \frac{2}{K_J^{1,2}}\right)\left[M_{J,u} - \left(M_{1,u}/\rho_1 + (M_{2,u} - M_{1,u}\rho_2/\rho_1)/\tilde{\rho}_2\right)\right] \end{aligned}$$

where $K_J^{(1,2)} = k_3$, is the new elastic flexural stiffness at the beam-to-column node.

The overall rotation is

$$\begin{aligned} \theta_{ms,u}^{(1,2,J)} &= \theta_{ms,u}^{(1)} + \Delta\theta_{ms,u}^{(1,2)} + \Delta\theta_{ms,u}^{(1,2,J)} = \\ &= \left(\frac{L}{3EI} + \frac{2}{K_J}\right)\frac{M_{1,u}}{\rho_1} + \left(\frac{L}{3EI} + \frac{2}{K_J^1}\right)\frac{M_{2,u} - M_{1,u}\rho_2/\rho_1}{\tilde{\rho}_2} + \\ &+ \left(\frac{L}{3EI} + \frac{2}{K_J^{1,2}}\right)\left[M_{J,u} - \left(M_{1,u}/\rho_1 + (M_{2,u} - M_{1,u}\rho_2/\rho_1)/\tilde{\rho}_2\right)\right] - \frac{2L}{3EI}M_{ms,u} \end{aligned} \tag{A2.2}$$

– Case C: hinges on elements $i = 1, 2, 3$

After hinges in elements $i = 1, 2$, it is possible to collapse when a further hinge forms at element $i = 3$; in this case we have a "joint rotation mechanism" with a failure load given by

$$q_{f,\bar{M}_R} = \frac{8\left(\bar{M}_R + M_{ms,u}\right)}{L^2} \tag{A2.3}$$

where

$$\bar{M}_R = \sum_{r=1}^{3} M_{r,J,u} \tag{A2.4}$$

with $M_{J,u} > \bar{M}_R$.

In order to obtain this mechanism from previous condition, it is necessary to increase the moment at the element $i = 3$

$$\Delta M_{3,J} = M_{3,u} - M_{1,u}(\rho_3/\rho_1) - (M_{2,u} - M_{1,u}\rho_2/\rho_1)\left(\tilde{\rho}_3/\tilde{\rho}_2\right)$$

so that the increment of beam-end section is $\Delta M_3 = \Delta M_{3,J}$. The total required rotation is

$$\begin{aligned}\theta_{ms,u}^{(1,2,3)} &= \theta_{ms,u}^{(1)} + \Delta\theta_{ms,u}^{(1,2)} + \Delta\theta_{ms,u}^{(1,2,3)} = \\ &= \left(\frac{L}{3EI} + \frac{2}{K_J}\right)\frac{M_{1,u}}{\rho_1} + \left(\frac{L}{3EI} + \frac{2}{K_J^1}\right)\frac{M_{2,u} - M_{1,u}\rho_2/\rho_1}{\tilde{\rho}_2} + \\ &+ \left(\frac{L}{3EI} + \frac{2}{K_J^{1,2}}\right)\left[M_{3,u} - M_{1,u}(\rho_3/\rho_1) - (M_{2,u} - M_{1,u}\rho_2/\rho_1)\left(\tilde{\rho}_3/\tilde{\rho}_2\right)\right] - \frac{2L}{3EI}M_{ms,u}\end{aligned} \tag{A2.5}$$

Appendix C. List of symbols

M_J - moment at the beam-end, see Fig. 1
$M_{J,u}$ - ultimate moment at the beam-end
M_{ms} - moment at beam mid-span, see Fig. 1
$M_{ms,u}$ - ultimate moment at beam mid-span
$M_{i,J}$ - moment at the i element-end, see Fig. 1
$M_{i,J,u} = M_{i,u}$ - ultimate moment at the i element-end
$M_{w,J,u}$ - ultimate moment at the beam-end relative to the weakest adjacent element failure
K_J - overall elastic flexural stiffness at the node due to the adjacent elements $i = 1, 2, 3$
$q_{J,u}$ - load that produces the first plastic hinge at beam-ends
$q_{ms,u}$ - load that produces the first plastic hinge at mid-span
$q_{w,J,u}$ - load that produces the first plastic hinge at the weakest adjacent element
V_u - beam–column joint ultimate shear
$M_{V,J,u}$ - ultimate beam moment at the beam-end that produces the joint shear failure
$q_{V,J,u}$ - load that produces the joint shear failure
q_f - failure load (plastic hinges at the beam-end section and beam mid-span)
$\theta_{J,u}$ - required rotation at the beam-end to achieve q_f
$\theta_{ms,u}$ - required rotation at beam mid-span to achieve q_f
$\theta_{J,u,eff}$ - effective rotation at the beam-end
$\theta_{ms,u,eff}$ - effective rotation at the beam mid-span
$q_{f,eff,J}$ - effective failure load due to the effective rotation $\theta_{J,u,eff}$
$q_{f,eff,ms}$ - effective failure load due to the effective rotation $\theta_{ms,u,eff}$
$\theta_{ms,u}^{(1,J)}$ - mid-span required rotation - collapse of 1-element and beam-end
$\theta_{ms,u}^{(1,2,J)}$ - mid-span required rotation - collapse of 1,2-elements and beam-end
$\theta_{ms,u}^{(1,2,3)}$ - mid-span required rotation - collapse of adjacent elements
$q_{f,\check{M}_R}$ - failure load - plastic hinges at beam mid-span and all adjacent elements

References

[1] N. Mitra, An Analytical Study of Reinforced Concrete Beam-Column Joint Behavior Under Seismic Loading (Ph. D. Thesis), Department of Civil and Environmental Engineering, University of Washington, 2007.
[2] N. Fardis, An european perspective to performance-based seismic design, assessment and retrofitting, in: Proceedings of International Workshop, Performance-Based Seismic Design Concepts and Implementation. Bled, Slovenia, 28 June - 1 July 2004.
[3] C.A. Pagni, L.N. Lowes, Tools to enable prediction of the economic impact of earthquake damage in older RC beam-column joints, in: Proceedings of International Workshop, Performance-Based Seismic Design Concepts and Implementation. Bled, Slovenia, 28 June - 1 July 2004.
[4] M. Pokhrel, J. Bandelt, Plastic hinge behavior and rotation capacity in reinforced ductile concrete flexural members, Eng. Struct. 200 (2019) 1–20.
[5] M. Scalvenzi, F. Parisi, Progressive collapse capacity of a gravity-load designed RC building partially collapsed during structural retrofitting, Eng. Fail. Anal. 121 (2021).
[6] D. D'Angela, G. Magliulo, F. Celano, E. Cosenza, Characterization of local and global capacity criteria for collapse assessment of code–conforming RC buildings, Bull. Earthq. Eng. 19 (2021) 3701–3743.
[7] Z. Xi, Z. Zhang, W. Qin, P. Zhang, Experiments and a reverse-curved compressive arch model for the progressive collapse resistance of reinforced concrete frames, Eng. Fail. Anal. 135 (2022) 106054.
[8] Eurocode 8, Design of Structures for Earthquake Resistance - Part 3: Assessment and Retrofitting of Buildings, BS EN 1998-3, 2005.
[9] NTC 2018, Norme Tecniche Per Le Costruzioni, Ministero delle Infrastrutture (2018). DM 17-01-2018.
[10] E. Maiorana, C. Denis Tetougueni, P. Zampieri, Effect of blast load on the structural integrity of steel arch bridge slab, Eng. Fail. Anal. 139 (2022) 106498.
[11] P. Foraboschi, Falling mass bearing capacity of reinforced concrete beams, Eng. Fail. Anal. 138 (2022) 106396.
[12] S. Elkoly, B. El-Ariss, Progressive collapse evaluation of externally mitigated reinforced concrete beams, Eng. Fail. Anal. 40 (2014) 33–34.
[13] H.M. Elsanadedy, Y.A. Al-Salloum, T.H. Almusallam, T. Ngo, H. Abbas, Progressive collapse evaluation of externally mitigated reinforced concrete beams, Eng. Fail. Anal. 105 (2019) 896–918.
[14] M. Valente, G. Milani, Alternative retrofitting strategies to prevent the failure of an under-designed reinforced concrete frame, Eng. Fail. Anal. 89 (2018) 271–285.
[15] T. Paulay, M.J.N. Priestley, Seismic Design of Reinforced Concrete and Masonry Buildings, Wiley New York, 1992.

[16] Eurocode 2, Design of Concrete Structures, European Committee for Standardization EN 1992, 2004.
[17] A. Borghini, F. Gusella, A. Vignoli, Seismic vulnerability of existing R.C. buildings: A simplified numerical model to analyse the influence of the beam-column joints collapse, Eng. Struct. 121 (2016) 19–29.
[18] A.C. Birely, L.N. Lowes, D.E. Lehman, A model for the practical nonlinear analysis of reinforced-concrete frames including joint flexibility, Eng. Struct. 34 (2012) 455–465.
[19] F. Vecchio, M. Collins, Investigating the collapse of a warehouse, Concr. Int. 12 (3) (1990) 72–78.
[20] S. Pantazopoulou, J. Bonacci, Consideration of questions about beam-column joints, ACI Struct. J. 89 (1) (1992) 27–36.
[21] S. Pampanin, G. Calvi, M. Moratti, Seismic behaviour of R.C. beam-column joints designed for gravity loads, in: 12th European Conference on Earthquake Engineering, London, 2002.
[22] A. Masi, G. Santarsiero, G. Lignola, G.M. Verderame, Study of the seismic behavior of external RC beam-column joints through experimental tests and numerical simulations, Eng. Struct. 52 (2013) 207–219.
[23] C. Cosgun, A.M. Turk, A. Mangir, T. Cosgun, G. Kiymaz, Experimental behaviour and failure of beam-column joints with plain bars, low-strength concrete and different anchorage details, Eng. Fail. Anal. 109 (2020).
[24] F. Gusella, M. Orlando, K.D. Peterman, On the required ductility in beams and connections to allow a redistribution of moments in steel frame structures, Eng. Struct. 179 (2019) 595–610.
[25] S.E. El-Metwally, W.F. Chen, Moment-rotation modeling of reinforced beam-column connections, ACI Struct. J. 85 (4) (1988) 384–394.
[26] S. Alath, S. Kunnath, Modeling inelastic shear deformation in rc beam-column joints, in: Tenth Conference on Engineering Mechanics, University of Colorado, Boulder, 1995, pp. 822–825.
[27] S.K. Kunnath, The genesis of IDARC and advances in macromodeling for nonlinear analysis of RC structures, Geotech., Geol. Earthq. Eng. 33 (2015) 29–42.
[28] M. Anderson, D. Lehman, J. Stanton, A cyclic shear stress–strain model for joints without transverse reinforcement, Eng. Struct. 30 (4) (2008) 941–954.
[29] A. Ghobarah, A. Biddah, Dynamic analysis of reinforced concrete frames including joint shear deformation, Eng. Struct. 21 (11) (1999) 971–987.
[30] M. Elmorsi, M.R. Kianoush, W.K. Tso, Modeling bond-slip deformations in reinforced concrete beam-column joints, Can. J. Civil Eng. 27 (3) (2000) 490–505.
[31] M. Youssef, A. Ghobarah, Strength deterioration due to bond slip and concrete crushing in modeling of reinforced concrete members, ACI Struct. J. 96 (6) (2000) 956–966.
[32] M. Shin, J.M. Lafave, Modeling of cyclic joint shear deformation contributions in RC beam-column connections to overall frame behavior, Struct. Eng. Mech. 18 (5) (2004) 645–669.
[33] S. Tajiri, H. Shiohara, F. Kusuhara, A new macroelement of reinforced concrete beam column joint for elasto-plastic plane frame analysis, in: Eighth National Conference of Earthquake Engineering, San Francisco, California, 2006.
[34] L.N. Lowes, N. Mitra, A. Altoontash, A beam-column joint model for simulating the earthquake response of reinforced concrete frames, in: Eighth National Conference of Earthquake Engineering, San Francisco, California, 2003.
[35] A. Altoontash, G.D. Deierlein, A Versatile Model for Beam–Column Joints, ASCE Structures Congress - Seattle - WA, 2003.
[36] L.N. Lowes, A. Altoontash, Modeling reinforced-concrete beam-column joints subjected to cyclic loading, J. Struct. Eng. 129 (12) (2003) 1686–1697.
[37] N. Mitra, L.N. Lowes, Evaluation, calibration, and verification of a reinforced concrete beam-column joint model, J. Struct. Eng. 133 (1) (2007) 105–120.
[38] J.-S. Jeon, L.N. Lowes, R. DesRoches, I. Brilakis, Fragility curves for non-ductile reinforced concrete frames that exhibit different component response mechanisms, Eng. Struct. 85 (2015) 127–143.
[39] H. Korkmaz, A. Yakut, A. Bayraktar, Analysis of a multi-story reinforced concrete residential building damaged under its self-weight, Eng. Fail. Anal. 98 (2019) 38–48.
[40] P. Foraboschi, Bending load-carrying capacity of reinforced concrete beams subjected to premature failure, Materials 12 (19) (2019).
[41] M. De Stefano, R. Nudo, G. Sarà, S. Viti, Effects of randomness in steel mechanical properties on rotational capacity of RC beams, Mater. Struct./Materiaux et Construct. 34 (2001) 92–99.
[42] SAP 2000, CSI Analysis Reference Manual for SAP 2000, Computers and Structures Inc, Berkeley, CA, 2022.